13

Wind Energy

Chaouki Ghenai and Armen Sargsyan
Ocean and Mechanical Engineering Department,
College of Engineering and Computer Science, Florida Atlantic University
Boca Raton, Florida,
U.S.A.

1. Introduction

1.1 Sustainable energy systems

Sustainable energy is to provide the energy that meets the needs of the present without compromising the ability of future generations to meet their needs. Sustainable energy has two components: renewable energy and energy efficiency. Renewable energy uses renewable sources such biomass, wind, sun, waves, tides and geothermal heat. Renewable energy systems include wind power, solar power, wave power, geothermal power, tidal power and biomass based power. Renewable energy sources, such as wind, ocean waves, solar flux and biomass, offer emissions-free production of electricity and heat. For example, geothermal energy is heat from within the earth. The heat can be recovered as steam or hot water and use it to heat buildings or generate electricity. The solar energy can be converted into other forms of energy such as heat and electricity and wind energy is mainly used to generate electricity. Biomass is organic material made from plants and animals. Burning biomass is not the only way to release its energy. Biomass can be converted to other useable forms of energy, such as methane gas or transportation fuels, such as ethanol and biodiesel (clean alternative fuels).

In addition to renewable energy, sustainable energy systems also include technologies that improve energy efficiency of systems using traditional non renewable sources. Improving the efficiency of energy systems or developing cleaner and efficient energy systems will slow down the energy demand growth, make deep cut in fossil fuel use and reduce the pollutant emissions. For examples, advanced fossil-fuel technologies could significantly reduce the amount of CO2 emitted by increasing the efficiency with which fuels are converted to electricity. Options for coal include integrated gasification combined cycle (IGCC) technology, ultra-supercritical steam cycles and pressurized fluidized bed combustion. For the transportation sector, dramatic reductions in CO2 emissions from transport can be achieved by using available and emerging energy-saving vehicle technologies and switching to alternative fuels such as biofuels (biodiesel, ethanol). For industrial applications, making greater use of waste heat, generating electricity on-site, and putting in place more efficient processes and equipment could minimize external energy demands from industry. Advanced process control and greater reliance on biomass and biotechnologies for producing fuels, chemicals and plastics could further reduce energy use and CO2 emissions. Energy use in residential and commercial buildings can be substantially

reduced with integrated building design. Insulation, new lighting technology and efficient equipment are some of the measures that can be used to cut both energy losses and heating and cooling needs. Solar technology, on-site generation of heat and power, and computerized energy management systems within and among buildings could offer further reductions in energy use and CO2 emissions for residential and commercial buildings.
The development of cleaner and efficient energy technologies and the use of new and renewable energy sources will play an important role in the sustainable development of a future energy strategy. The promotion of renewable sources of energy such as wind energy and the development of cleaner and more efficient energy systems are a high priority, for security and diversification of energy supply, environmental protection, and social and economic cohesion (International Energy Agency, 2006).

1.2 History about wind energy

The use of wind as an energy source begins in antiquity. Mankind was using the wind energy for sailing ships and grinding grain or pumping water. Windmills appear in Europe back in 12th century. Between the end of nineteenth and beginning of twentieth century, first electricity generation was carried out by windmills with 12 KW. Horizontal-axis windmills were an integral part of the rural economy, but it fell into disuse with the advent of cheap fossil-fuelled engines and then the wide spread of rural electrification. However, in twentieth century there was an interest in using wind energy once electricity grids became available. In 1941, Smith-Putnam wind turbine with power of 1.25 MW was constructed in USA. This remarkable machine had a rotor 53 m in diameter, full-span pitch control and flapping blades to reduce the loads. Although a blade spar failed catastrophically in 1945, it remains the largest wind turbine constructed for some 40 years (Acker and Hand, 1999). International oil crisis in 1973 lead to re-utilization of renewable energy resources in the large scale and wind power was among others. The sudden increase in price of oil stimulated a number of substantial government-funded programs of research, development and demonstration. In 1987, a wind turbine with a rotor diameter of 97.5 m with a power of 2.5MW was constructed in USA. However, it has to be noted that the problems of operating very large wind turbines, in difficult wind climates were underestimated. With considerable state support, many private companies were constructing much smaller wind turbines for commercial sales. In particular, California in the mid-1980's resulted in the installation of very large number of quite small (less than 100 KW) wind turbines. Being smaller they were generally easy to operate and also repair or modify. The use of wind energy was stimulated in 1973 by the increase of price of fossil-fuel and of course, the main driver of wind turbines was to generate electrical power with very low CO_2 emissions to help limit the climate change. In 1997 the Commission of the European Union was calling for 12 percent of the gross energy demand of the European Union to be contributed from renewable by 2010. In the last 25 years the global wind energy had been increasing drastically and at the end of 2009 total world wind capacity reached 159,213 MW as shown in Figure 1. Wind power showed a growth rate of 31.7 %, the highest rate since 2001. The trend continued that wind capacity doubles every three years. The wind sector employed 550,000 persons worldwide. In the year 2012, the wind industry is expected for the first time to offer 1 million jobs. The USA maintained its number one position in terms of total installed capacity and China became number two in total capacity, only slightly ahead of Germany, both of them with around 26,000 Megawatt of wind capacity installed. Asia accounted for the largest share of

new installations (40.4 %), followed by North America (28.4 %) and Europe fell back to the third place (27.3 %). Latin America showed encouraging growth and more than doubled its installations, mainly due to Brazil and Mexico. A total wind capacity of 203,000 Megawatt will be exceeded within the year 2010. Based on accelerated development and further improved policies, world wide energy association WWEA increases its predictions and sees a global capacity of 1,900,000 Megawatt as possible by the year 2020 (World Wide Energy Association report, 2009). The world's primary energy needs are projected to grow by 56% between 2005 and 2030, by an average annual rate of 1.8% per year (European Wind Energy Agency, 2006).

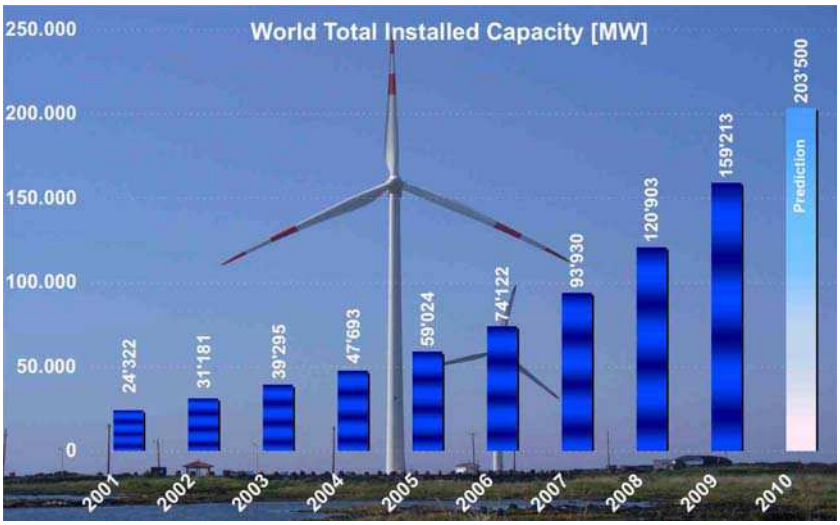

Fig. 1. World total installed capacity by the end of 2009 - Data source: wwea.org

1.3 Fundamental concepts of wind turbine systems

1.3.1 Type of wind turbines

A wind turbine is a rotary device that extracts the energy from the wind. The mechanical energy from the wind turbine is converted to electricity (wind turbine generator). The wind turbine can rotate through a horizontal (horizontal axis wind turbine – HAWT) or vertical (VAWT) axis (See Figure 2). Most of the modern wind turbines fall in these two basic groups: HAWT and VAWT. For the HAWT, the position of the turbine can be either upwind or downwind. For the horizontal upwind turbine, the wind hits the turbine blade before it hits the tower. For the horizontal downwind turbine, the wind hits the tower first (See Figure 2). The basic advantages of the vertical axis wind turbine are (1) the generator and gear box can be placed on the ground and (2) no need of a tower. The disadvantages of the VAWT are: (1) the wind speeds are very low close to ground level, so although you may save a tower, the wind speeds will be very low on the lower part of the rotor, and (2) the overall efficiency of the vertical axis wind turbine is not impressive (Burton et al., 2001).

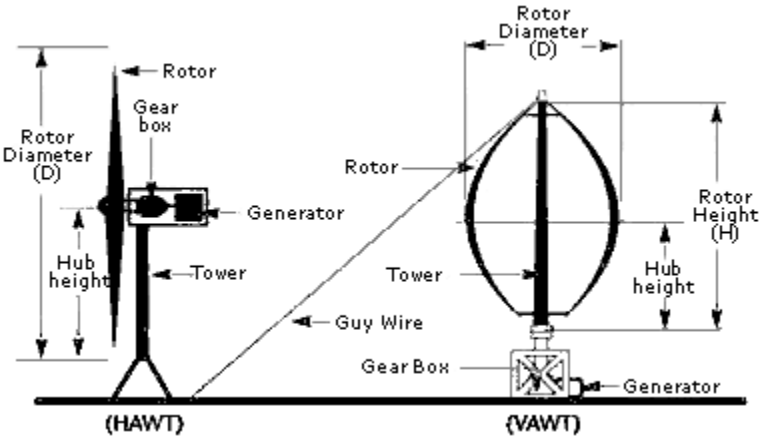

Fig. 2. Horizontal and vertical wind turbines

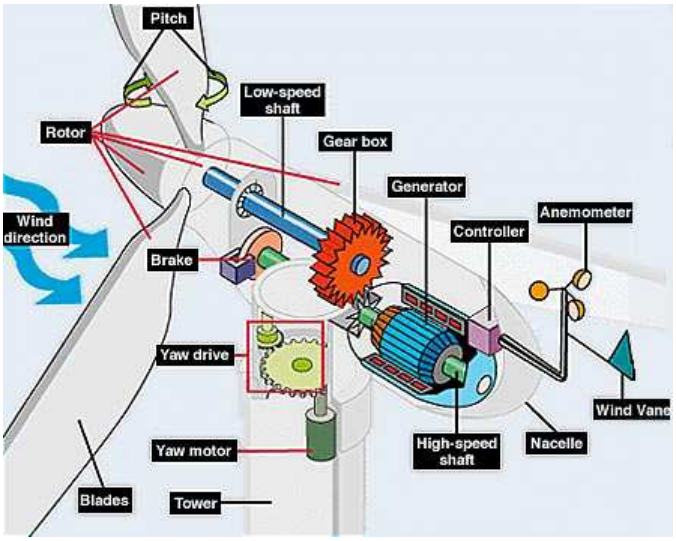

Fig. 3. Wind turbine parts

1.3.2 Wind turbine parts

The main parts of a wind turbine parts (see Figure 3) are:

- **Blades**: or airfoil designed to capture the energy from the strong and fast wind. The blades are lightweight, durable and corrosion-resistant material. The best materials are composites of fiberglass and reinforced plastic.
- **Rotor**: designed to capture the maximum surface area of wind. The rotor rotates the generator through the low speed shaft and gear box.
- **Gear Box**: A gear box magnifies or amplifies the energy output of the rotor. The gear box is situated directly between the rotor and the generator.

- **Generator:** The generator is used to produce electricity from the rotation of the rotor. Generators come in various sizes, relative to the desired power output.
- **Nacelle:** The nacelle is an enclosure that seals and protects the generator and gear box from the other elements.
- **Tower:** The tower of the wind turbine carries the nacelle and the rotor. The towers for large wind turbines may be either tubular steel towers, lattice towers, or concrete towers. The higher the wind tower, the better the wind. Winds closer to the ground are not only slower, they are also more turbulent. Higher winds are not corrupted by obstructions on the ground and they are also steadier.

1.3.3 Wind turbine design

During the design of wind turbines, the strength, the dynamic behavior, and the fatigue properties of the materials and the entire assembly need to be taken into consideration. The wind turbines are built to catch the wind's kinetic energy. Modern wind turbines are not build with a lot of rotor blades. Turbines with many blades or very wide blades will be subject to very large forces, when the wind blows at high speed. The energy content of the wind varies with the third power of the wind speed. The wind turbines are build to withstand extreme winds. To limit the influence of the extreme winds and to let the turbines rotates relativelly quickly it is generarlly prefer to build turbines with a few, long, narrow blades.

- **Fatigue Loads (forces)**: If the wind turbines are located in a very turbulent wind climate, they are subject to fluctuating winds and hence fluctuating forces. The components of the wind tubrine such as rotor blades with repeated bending may develop cracks which ultimately may make the component break. When designing a wind turbine it is important to calculate in advance how the different components will vibrate, both individually, and jointly. It is also important to calculate the forces involved in each bending or stretching of a component (structural dynamics).
- **Upwind/Downwind wind turbines designs:** The upwind wind turbines have the rotor facing the wind. The basic advantage of upwind designs is that one avoids the wind shade behind the tower. By far the vast majority of wind turbines have this design. The downwind wind turbines have the rotor placed on the lee side of the tower.
- **Number of blades:** Most modern wind turbines are three-bladed designs with the rotor position maintained upwind using electrical motors in their yaw mechanism. The vast majority of the turbines sold in world markets have this design. The two-bladed wind turbine designs have the advantage of saving the cost of one rotor blade and its weight. However, they tend to have difficulty in penetrating the market, partly because they require higher rotational speed to yield the same energy output.
- **Mechanical and aerodynamics noise:** sound emissions from wind turbines may have two different origins: Mechanical noise and aerodynamic noise. The mechanical noise originates from metal components moving or knocking against each other may originate in the gearbox, in the drive train (the shafts), and in the generator of a wind turbine. Sound insulation can be useful to minimise some medium- and high-frequency noise. In general, it is important to reduce the noise problems at the source, in the structure of the machine itself. The source of the aerodynamic sound emission is when the wind hits different objects at a certain speed, it will generally start making a sound. For example, rotor blades make a slight swishing sound at relatively low wind speeds.

Careful design of trailing edges and very careful handling of rotor blades while they are mounted, have become routine practice in the industry.

1.3.4 Wind turbine power

The Wind turbines work by converting the kinetic energy in the wind first into rotational kinetic energy in the turbine and then electrical energy. The wind power available for conversion mainly depends on the swept area of the turbine (see Figure 4):

$$P_W = \frac{1}{2}\rho A V^3 \tag{1}$$

Where ρ is the air density (Kg/m^3), A is the swept area (m^2) and V the wind speed (m/s).
Albert Betz (German physicist) concluded in 1919 that no wind turbine can convert more than 16/27 (59.3%) of the kinetic energy of the wind into mechanical energy turning a rotor (Betz Limit or Betz). The theoretical maximum power efficiency of any design of wind turbine is 0.59 (Hau, 2000 and Hartwanger and Horvat, 2008). No more than 59% of the energy carried by the wind can be extracted by a wind turbine. The wind turbines cannot operate at this maximum limit. The power coefficient C_p needs to be factored in equation (1) and the extractable power from the wind is given by:

$$P = \frac{1}{2}C_P \rho A V^3 \tag{2}$$

Example: Given the following data: Blade length l = 52 m, wind speed, V = 12m/s, air density ρ = 1.23 Kg/m^3 and power coefficient C_P = 0.4. Calculate the power converted from the wind into rotational energy in the turbine?
The swept area A = $\pi r^2 = \pi l^2 = 3.14 * 52^2 = 8495$ m^2
The available power P = ½ C_P ρ A V^3 = ½ x 1.23 x 8495 x 12^3 x 0.4 = 3.6 MW

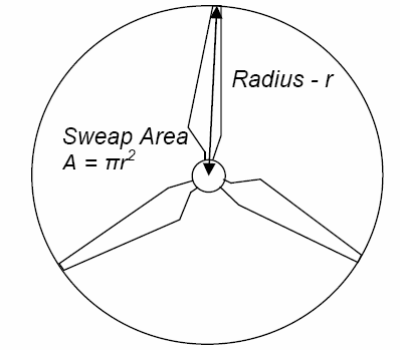

Fig. 4. Swept area of the wind turbine

1.3.5 Power coefficient Cp

The Cp value is unique to each turbine type and is a function of wind speed that the turbine is operating in. In real world, the value of C_p is well below the Betz limit (0.59) with values of 0.35 - 0.45 for the best designed wind turbines. If we take into account the other factors in

a complete wind turbine system (gearbox, bearings, generator), only 10-30% of the power of the wind is actually converted into usable electricity. The power coefficient C_p, defined as that the power extracted by rotor to power available in the wind is given by:

$$C_p = \frac{P}{\frac{1}{2}\rho A V^3} = \frac{Power\,Extracted\,by\;Rotor}{Power\,Available\,in\,the\,Wind} \tag{3}$$

The power coefficient C_P, defined as extracted power over the total available power can be similarly defined in terms of axial induction factor a (Hansen, 2000 and Hartwanger and Horvat, 2008) as:

$$C_p = 4a(1-a)^2 \tag{4}$$

The axial induction factor a is the fractional decrease in wind velocity between the free stream (Position 1) and rotor plane (Position 2) as shown in Figure 5. The axial induction factor can be expressed as:

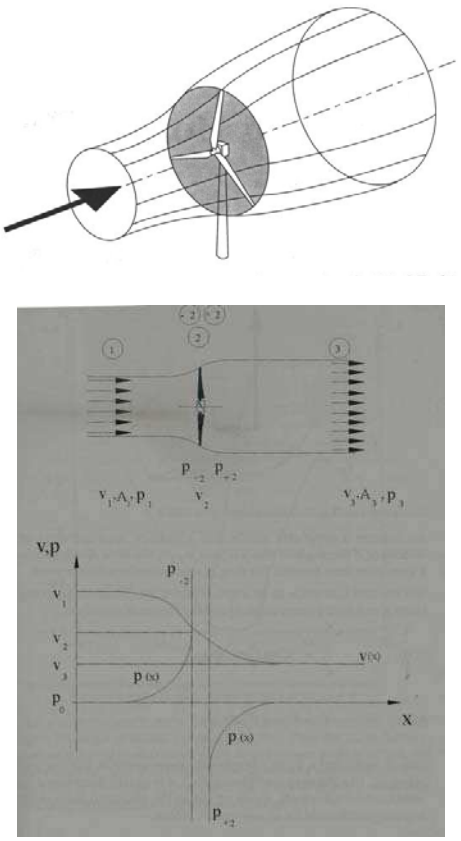

Fig. 5. Velocity and pressure distribution

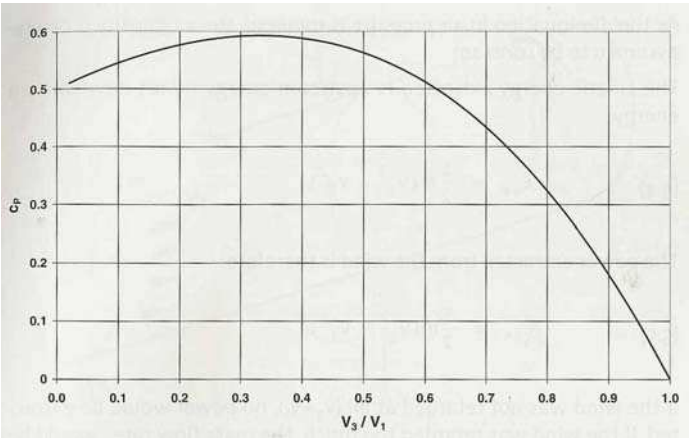

Fig. 6. Power coefficients Cp versus V3/V1 ratio

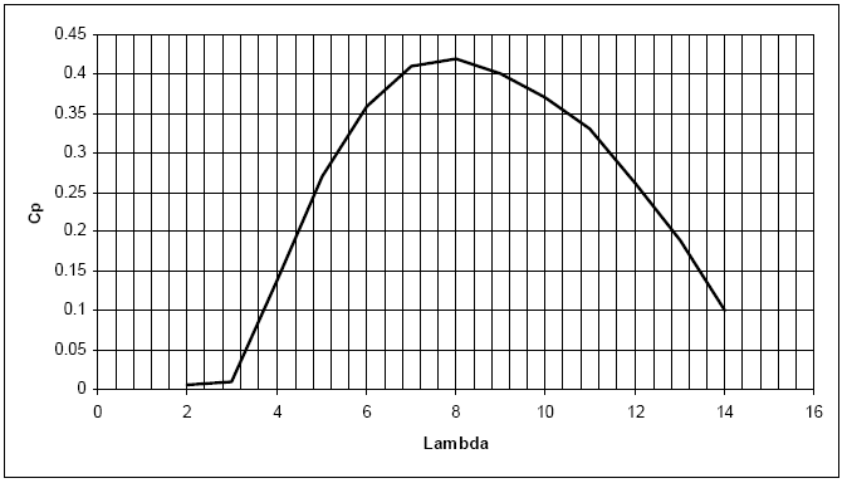

Fig. 7. Power coefficient Cp curve versus λ

$$a = \frac{V_1 - V}{V_1} \tag{5}$$

The velcoity V is defined by:

$$V = \frac{1}{2}\left(V_1 + V_3\right) \tag{6}$$

The variation of the power coefficient C_P versus the velocity ration V3/V1 is shown in Figure 6. The power coefficient C_P is not a static value. It varies with the tip speed ratio of the turbine (TSR or λ) as shown in Figure 7. The tip speed ratio is defined by ratio between the tip speed (tangential velocity) and the undisturbed wind speed V_1 entering the turbine:

$$\lambda = \frac{\Omega r}{V_1} \tag{7}$$

Where Ω is the rotational speed of the turbine and r is the length of the blade. The variation of the power coefficient C_P versus the tip speed ratio is shown in Figure 6.

1.3.6 Torque

The wind turbines extract power from the wind in mechanical form and transmit it to the load by rotating shafts. The shaft must be properly designed to transmit this power. When power is being transmitted through a shaft, a torque T (N.m/rad) will be present. This torque is given by:

$$T = \frac{P}{\Omega} \tag{8}$$

P is the mechanical power and Ω is the rotational speed or the turbine or the angular velocity (rad/s).

1.4 Characteristics of wind: wind power density, wind shear and turbulence

Wind resource evaluation is a critical element in projecting turbine performance at a given site. The energy available in a wind stream is proportional to the cube of its speed, which means that doubling the wind speed increases the available energy by a factor of eight. With a wind speed of 8 meters per second we get a power (amount of energy per second) of 314 Watts per square meter exposed to the wind (the wind is coming from a direction perpendicular to the swept rotor area). At 16 m/s we get eight times as much power, i.e. 2509 W/m^2. Further more the wind speed also varies with the time of day, season, height above ground, and type of terrain. Proper sitting in windy locations, away from large obstructions, enhances a wind turbine's performance. In general, annual average wind speeds of 5 meters per second (11 miles per hour) are required for grid-connected applications. Annual average wind speeds of 3 to 4 m/s (7-9 mph) may be adequate for non-connected electrical and mechanical applications such as battery charging and water pumping. Wind resources exceeding this speed are available in many parts of the world. The Wind Power Density (WPD) is a useful way to evaluate the wind resource available at a potential site. The wind power density, measured in watts per square meter, indicates how much energy is available at the site for conversion by a wind turbine. Classes of wind power density for two standard wind measurement heights are listed in the Table 1 below. Wind speed generally increases with height above ground. In general, sites with a wind power class rating of 4 or higher are now preferred for large scale wind turbines.

The wind shear is the sudden, drastic change in wind direction or speed over a comparatively short distance. Most winds travel horizontally, as does most wind shear, but under certain conditions, including thunderstorms and strong frontal systems, wind shear will travel in a vertical direction. With its sharp shifts in wind direction and relative wind speed, it can cause a reduction of wind turbine performance and may also cause damage to the wind turbine blades. The wind turbine must never be located such that it is subject to excessively wind shear and turbulent air flow. Light turbulence will decrease performance since a turbine cannot react to rapid changes in wind direction, while heavy turbulence may

reduce expected equipment life or result in wind turbine failure. Turbulence may be avoided by following a few basic rules: (1) the wind turbine should be mounted on a cleared site free from minor obstructions such as trees and buildings and (2) If it is not possible to avoid obstructions, tower height should be increased to a value of approximately 9 meters greater than the height of obstructions, and (3) A good "rule of thumb" is to locate the turbine at a minimum height of three times that of the tallest upwind barrier.

	10 meters		50 meters	
Wind Power class	Wind power density (W/m^2)	Speed (m/s)	Wind power density (W/m^2	Speed (m/s)
1	< 100	< 4.4	< 200	< 5.6
2	100- 150	4.4 – 5.1	200 – 300	5.6 – 6.4
3	150 – 200	5.1 – 5.6	300 - 400	6.4 – 7.0
4	200 – 250	5.6 – 6.0	400 - 500	7.0 – 7.5
5	250 – 300	6.0 - 6.4	500 – 600	7.5 – 8.0
6	300 – 400	6.4 – 7.0	600 – 800	8.0 – 8.8
7	> 400	> 7.0	> 800	> 8.8

Table 1. Classes of wind power density at two different wind measurements heights

1.5 Aerodynamics, flow structure in wind turbine wake and wind farm

Wind turbine aerodynamics of a horizontal-axis wind turbine (HAWT): The air flow at the blades is not the same as the airflow further away from the turbine. The very nature of the way in which energy is extracted from the air also causes air to be deflected by the turbine.

Flow Structure in wind turbine wake: The near region immediately downstream of the rotor, vortex sheets, associated with the radial variation in circulation along the blades, are shed from their trailing edge, and roll up in a short downstream distance forming tip vortices that describe helical trajectories (near wake region). When the inclination angle of the helix is small enough, the layer, in which the tip vortices are located, can be interpreted as a cylindrical shear layer which separates the slow moving fluid in the wake from that on the outside. Because of turbulent diffusion, the thickness of the shear layer increases with downstream distance. Most of the turbulence that makes the wake diffuse is, at this stage, created by the shear in the wake, mainly in the shear layer. However, the shear in the external atmospheric flow also plays an important role, at least in the redistribution of the generated turbulence. At a certain distance downstream about two to five diameters, the shear layer reaches the wake axis. This marks the end of the near wake region. After the near wake region, there is a transition region leading to the far wake region, where the wake is completely developed and, in the hypothetical absence of ambient shear flow, it may be assumed that the perturbation profiles of both velocity deficit and turbulence intensity are axisymmetric, and have self-similar distributions in the cross-sections of the wake. This property of self-similarity is the basis of the kinematic models describing wind turbine wakes.

Wind Farm: A wind farm is as a cluster of wind turbines that acts and is connected to the power system as a single electricity producing power station. Generally it is expected that a wind farm consists of more than three wind turbines. Modern wind farms may have capacities in the order of hundreds of megawatts, and are installed offshore as well as on

land. Modern wind farms generally are connected to the high voltage transmission system, in contrast to the early application of wind energy for electricity production with wind turbines individually connected to the low- to medium-voltage distribution system. Hence, modern wind farms are considered power plants with responsibilities for control, stability, and power balance. Most of the other technical issues with wind farms are associated with the close spacing of multiple turbines. The close spacing implies that extraction of energy by wind turbines upwind will reduce the wind speed and increase the turbulence, which may cause reduced efficiency and higher loads on downwind turbines. Another technical issue for large wind farms is the grid connection and the integration into the power system. Large wind farms are very visible, especially at land and in coastal areas and this together with a number of environmental concerns, such as possible disturbance of migrating birds and bats, play an important role in the wind farm planning process and can result in selection of sites with less than optimal wind conditions.

1.6 Commercial wind turbines

Commercial wind farms are constructed to generate electricity for sale through the electric power grid. The number of wind turbines on a wind farm can vary greatly, ranging from a single turbine to thousands. Large wind farms typically consist of multiple large turbines located in flat, open land. Small wind farms, such as those with one or two turbines, are often located on a crest or hill. The size of the turbines can vary as well, but generally they are in the range of 500 Kilowatts to several Megawatts, with 4.5 Megawatts being about the largest. Physically, they can be quite large as well, with rotor diameters ranging from 30 m to 120 m and tower heights ranging from 50 m to 100 m. The top ten wind turbine manufacturers, as measured by global market share in 2007 are listed in Table 2. Due to advances in manufacturing and design, the larger turbines are becoming more common. In general, a one Megawatt unit can produce enough electricity to meet the needs of about 100-200 average homes. A large wind farm with many turbines can produce many times that amount. However, with all commercial wind farms, the power that is generated first flows into the local electric transmission grid and does not flow directly to specific homes.

		Model	Power rating [kW]	Diameter [m]	Tip speed [m/s]
1	Vestas	V90	3,000	90	87
2	GE Energy	2.5XL	2,500	100	86
3	Gamesa	G90	2,000	90	90
4	Enercon	E82	2,000	82	84
5	Suzlon	S88	2,100	88	71
6	Siemens	3.6 SWT	3,600	107	73
7	Acciona	AW-119/3000	3,000	116	74.7
8	Goldwind	REpower750	750	48	58
9	Nordex	N100	2,500	99.8	78
10	Sinovel	1500 (Windtec)	1,500	70	

Table 2. Top ten wind commercial wind turbines manufactures in 2007

2. Three dimensional modelling of flow field of Horizontal Axis Wind Turbine (HAWT) using RANS method

Full three-dimensional computations, employing the Reynolds averaged Navier Stokes (RANS) equations, have been carried out by Kang and Hirsh (2001), focused on 3-D effects on a HAWT. They have used the EURANUS/Turbo solver with either algebraic and k–ω turbulence models for closure. Several numerical investigations were carried out on HAWT, using in-house Navier-Stokes solver EllipSys2D/3D, and dealing with overall performances, loads, design of rotors and blade sections (Sorensen, 2002, 2004 and 2005). Commercial CFD package Fluent was used to perform a detailed analysis of HAWT flow (Carcangiu, 2007). The steady flow field around an isolated rotor of a middle-sized HAWT was predicted in a non-inertial reference frame, using both the Spalart-Allmaras turbulence model and the κ–ω SST model, and specifying a constant axial wind velocity at the inlet. The classical BEM method was adopted for the design of a first turbine model, extending the active part of the blade close to the hub. This blade region is aerodynamically redesigned following the tendencies of modern wind turbines (Rohden, 2004). Several 2D and 3D simulations were carried out, to yield information on the different aspects involved by this problem, ranging from performance calculations to wake development.
The principal objective of this computaional fluid dynamics (CFD) analysis is to investigate the flow field around a horizontal axis wind turbine rotor and to determine the turbine's power over a full range of operating conditions (wind speed and rotational speed of the turbine). A three dimesional CFD analysis was performed in this study using Reynolds Averaged Navier Stokes (RANS) method. Due to periodicity of the wind turbine, only one third of the turbine rotor was modeled, and a single moving reference frame system (SMRF) was used in this study. The turbulnece was modeled using k-ε turbulene model. The governing equations of mass, mometum and turbulence equations were solved using finite volume method. The numerical results of the wind turbine coefficient of performance were compared to the experimetal data for the validation of the model. The results of the CFD analysis include the velocity field (x-velocity, y-velocity, z-velocity, and velocity magnitude), pressure distribution around the wind turbine blades, turbulent wake behind the wind turbine and the power coefficient C_P.

2.1 Governing equations

The mathematical equations describing the aerodynamics of wind turbines are based on the equations of conservation of mass and momentum together with other supplementary equations for the turbulence. The standard k-ε turbulence model is used in this study. The equations for the turbulent kinetic energy k and the dissipation rate of the turbulent kinetic energy ε are solved. The time averaged gas phase equations for steady turbulent flow are:

$$\frac{\partial}{\partial x_j}\left(\rho u_i \Phi\right) = -\frac{\partial}{\partial x_i}\left(\Gamma_\Phi \frac{\partial \phi}{\partial x_i}\right) + S_\Phi \tag{9}$$

Where ϕ is the dependent variable that can represent the velocity u_i, the turbulent kinetic energy k, and the dissipation rate of the turbulent kinetic energy ε .

2.1.1 Continuity equation

The equation of conservation of mass or continuity equation is given by:

$$\frac{\partial}{\partial x_j}\left(\rho u_i\right)=0 \tag{10}$$

2.1.2 Momentum equation

The Momentum equation is given by:

$$\frac{\partial\left(\overline{\rho u_i u_j}\right)}{\partial x_j}=-\frac{\partial \bar{P}}{\partial x_i}+\frac{\partial\left(\overline{t_{ij}}+\overline{\tau_{ij}}\right)}{\partial x_j} \tag{11}$$

Where, $\overline{t_{ij}}$ is the viscous stress tensor defined as:

$$\bar{t}_{ij}=\mu\left[\left(\frac{\partial \overline{u_i}}{\partial x_j}+\frac{\partial \overline{u_j}}{\partial x_i}\right)-\frac{2}{3}\frac{\partial \overline{u_k}}{\partial x_k}\delta_{ij}\right] \tag{12}$$

Where $\delta_{ij}=1 \;\; if \;\; i=j \;\; and \;\; \delta_{ij}=0 \;\; if \;\; i\neq j$

$\bar{\tau}_{ij}=-\overline{\rho\, u_i^{'}\, u_j^{'}}$ is the average Reynolds stress tensor defined as:

$$\overline{\tau_{ij}}=\mu_t\left[\left(\frac{\partial \overline{u_i}}{\partial x_j}+\frac{\partial \overline{u_j}}{\partial x_i}\right)-\frac{2}{3}\frac{\partial \overline{u_k}}{\partial x_k}\delta_{ij}\right]-\frac{2}{3}\left(\overline{\rho k\,\delta_{ij}}\right) \tag{13}$$

Where, $\bar{k}=\frac{1}{2}\overline{u_i u_j}$ is the average turbulent kinetic energy, $\mu_t=c_\mu\frac{\overline{\rho\, k^2}}{\bar{\varepsilon}}$ is the turbulent eddy viscosity, c_μ is constant (c_μ=0.09) and $\bar{\varepsilon}=\nu\overline{\frac{\partial u_i^{'}}{\partial x_j}\frac{\partial u_i^{'}}{\partial x_j}}$ is the average dissipation rate of the turbulent kinetic energy.

2.1.3 Transport equations for k and ε:

The standard k-ε model is a semi-empirical model based on model transport equations for the turbulence kinetic energy k and its dissipation rate ε:

2.1.3.1 Turbulent kinetic energy equation:

$$\rho\frac{\partial\left(\overline{k\,u_j}\right)}{\partial x_j}=\frac{\partial\left[\left(\mu+\frac{\mu_t}{\sigma_k}\right)\frac{\partial \bar{k}}{\partial x_j}\right]}{\partial x_j}+G_k-\overline{\rho\,\varepsilon} \tag{14}$$

Where, σ_k=1 and G_k is the production of turbulent kinetic energy defined as:

$$G_K=\mu_t\left[\left(\frac{\partial \overline{u_i}}{\partial x_j}+\frac{\partial \overline{u_j}}{\partial x_i}\right)\right]\frac{\partial \overline{u_i}}{\partial x_j}-\frac{2}{3}\frac{\partial \overline{u_i}}{\partial x_j}\delta_{ij}\left[\mu_t\frac{\partial \overline{u_k}}{\partial x_k}+\overline{\rho\, k}\right] \tag{15}$$

2.1.3.2 Dissipation of kinetic energy

$$\rho\frac{\partial\left(\overline{\varepsilon\, u_j}\right)}{\partial x_j}=C_{\varepsilon 1}\frac{\overline{\varepsilon}}{k}G_k+\frac{\partial\left[\left(\mu+\frac{\mu_t}{\sigma_\varepsilon}\right)\frac{\partial\overline{\varepsilon}}{\partial x_j}\right]}{\partial x_j}-C_{\varepsilon 2}\overline{\rho}\frac{\overline{\varepsilon^2}}{k} \tag{16}$$

Where C_{ε_1} = 1.44, C_{ε_2} = 1.92, σ_ε =1.3

2.2 Geometry, mesh, boundary conditions and numerical method

The equation of fluid flow is usually solved in stationary (or inertial) reference frames. However, there are many fluid flow problems that require the equations be solved in a moving (or non-inertial) reference frames. Rotating rotor of wind turbine is such case. There are two types of moving frames: multiple reference frames (MRF – different regions in the computational domain are rotating with different speed) and a single reference frame (the entire computational domain is rotating with the same speed). The single reference frame is used in this study. Table 3 shows the wind turbine blade characteristics used for this study. The wind turbine has three blades and a turbine rotor diameter of 6 m. The foil series which was used for the blade design was the NACA 638xx. The computational domain is extended in axial direction roughly 2 diameter upstream and 5 diameters downstream of the rotor (See Figure 8). In the vertical plane of the rotor, the cylindrical domain diameter is 1.5 times of the rotor diameter. ANSYS ICEM CFD 12 was used to build a tetrahedral mesh with approximately 870,000 volume elements. Periodic section of the hub and the blade was modeled. By applying periodicity, high number of mesh elements are used for 1/3 sector of the computational domain (See Figure 9), which will produce more accurate results.

Rotor radius	3m
Blade length	2.625m
Hub radius	0.375m
Number of blades	3
Twist	15 degree
Foil Type	NACA 638xx

Table 3. Characteristics of the investigated turbine

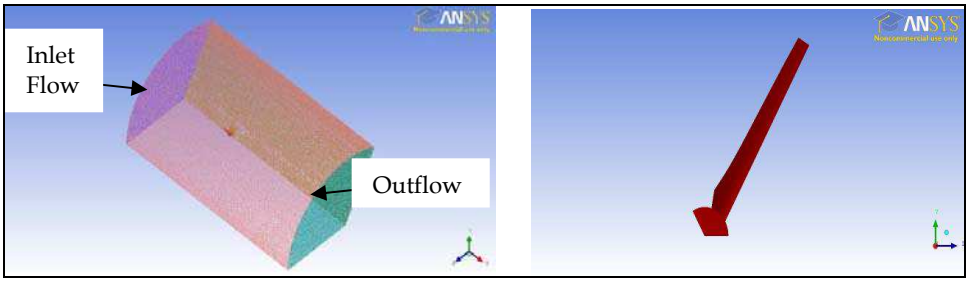

Fig. 8. Three dimensional computational domain and blade model

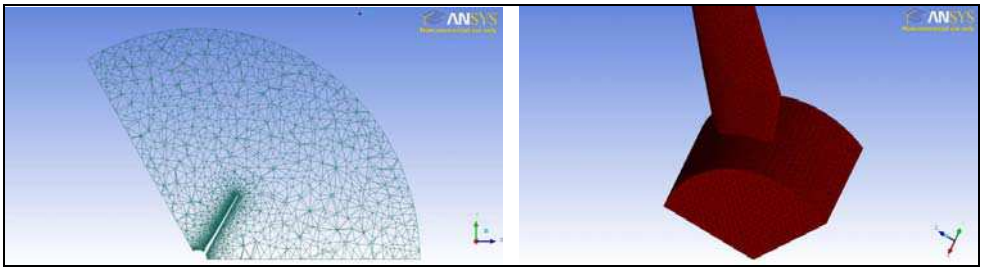

Fig. 9 Mesh generated (a) 2-D view of the mesh generated for the computational domain and (b) mesh created on the surface of the blade and hub

After creating a 3-D geometry model and generating the mesh, the flow boundary conditions (BC) have to be specified as shown in Figure 10. It is a very critical for simulation, that these boundary conditions are specified appropriately: (1) Wall (no-slip) boundary conditions are used for the blade surface and hub, (2) Velocity-inlet: This BC is used to specify the air flow velocity, (3) Outflow: Outflow boundary condition is used to model flow exits (the mass flow rate through the inlet BC should be the same as the flow arte through the outflow BC), (4) Symmetry: symmetry boundary conditions (zero flux of all quantities across the symmetry boundary) are used for the outer diameter of the cylindrical region representing the limit of the computational domain), (5) periodic: periodic boundary condition is used since only one third of the turbine blade is modeled. Periodic boundary conditions are used when the physical geometry of interest and the expected pattern of the flow/thermal solution have a periodically repeating nature. By using a periodic boundary the number of grids can be reduced enabling finer grids. Figure 10 shows the two dimensional views (the full blade and $1/3^{rd}$ of the turbine blade) of the wind turbine with the corresponding boundary conditions. The velocity inlet and outflow boundaries are shown in Figure 8.

For the numerical method, the finite volume method and the first order upwind method were used to solve the governing equations. The convergence criteria were set to 10^{-3} for the continuity, momentum, turbulent kinetic energy, and dissipation rate of the turbulent kinetic energy.

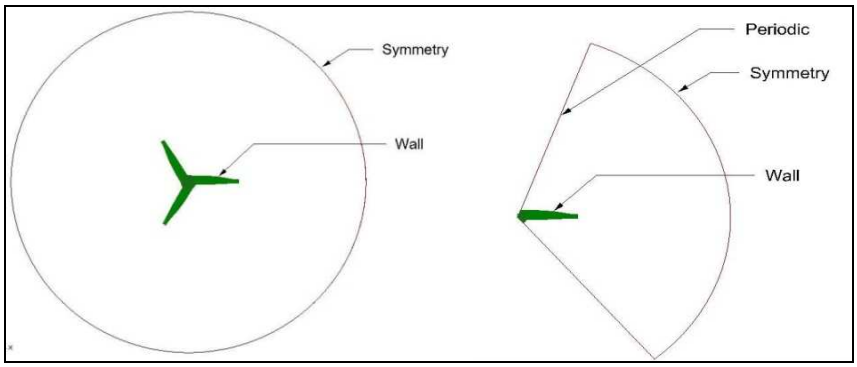

Fig. 10. Two dimensional views of the wind turbine, computational domain and boundary conditions

2.3 Results

The flow field around the wind turbine was predicted for a tip speed ratio TSR = 7, inlet wind speed of 10 m/s and the blade rotational speed of 26.66 rad/s. The axial, radial and tangential velocity contours are obtained at different sections along the x axis (flow direction). Figure 11 shows the normalized axial velocity (Vx/Vo) contours at different axial positions x/d = -1 to 3. The contours are plotted by taking clipped surface from the center of the hub to a radially outward distance of 4 m. This allows visualizing the contours close to near-blade region. The results show that the wind speed velocity decreases as the flow approaches the rotor because of the backflow effect. According to actuator disk theory axial velocity is reduced at the rotor plane (due to induction factor) in the presence of the rotor and it is confirmed in x/d=0 contour.

Figure 12 shows the wake expansion along the flow at y = 0 inclined plane, which cuts through the turbine blade at angle of 60^o to the z-axis. As flow moves downstream, it can be seen that wake expands along the direction of the flow. However, magnitude of velocity decreases within the stream tube. Green area right after the turbine indicates very low and even negative velocities because of hub bluntness. Light yellow area corresponds to velocity magnitude of about 6.17 m/s at the outflow, which kept at distance of 5D after the rotor. The wake field boundary shows a smoother gradient and the far wake is dominated by diffusion phenomena, so that the wake is forced by external flow. It is of interest to know the turbulence characteristics in wind farms in order to predict the mechanical loads on the wind turbines and their performances and to evaluate the velocity deficit created in the wind stream by the drag of the turbines. A distinct division can be made into near and far wake region. The near wake is taken as the region just behind the rotor, where the properties of the rotor flow can be noticeably discriminated, roughly up to one rotor diameter downstream. In this region the presence of the rotor is visible because of the aerodynamic perturbation created by the blades, including stalled flow, three dimensional effects and tip vortices. The near wake survey is focused on the physical process of energy conversion. The far wake is the region beyond the near wake, where the focus is put on the mutual influence of wind turbines in farm situations. The main research interest is to study how the far wake decays down-stream, in order to estimate the effects produced on the downstream turbines, i.e. lower velocity and higher turbulence intensity, which make the power production decrease and the unsteady loads increase. This observation is helpful in means of positioning next turbine when wind farm considered and it is clear that 5D distances is not enough. More deep far wake studies are required for such determination.

Figure 13 shows the normalized axial velocity plots at various x/d locations taken at radial lines inclined at the angle of 60^o to the z-axis. Here also it can be observed the fact that axial velocity gets reduced before the turbine and geometry of the hub (bluntness) also accounts for zero or sub-zero velocities downstream of the rotor. The expansion of the wake can be visualized where velocity reaches the stream velocity V_0 and shifts further outward radially as the flow advances.

Figure 14 shows the contours of the normalized tangential velocities. As it can be observed from the contour plots, variations of tangential velocity vectors starts about at x/d = - 0.05 to x/d = 0.5. It is also noted that the tangential velocity at the tip of the blade reached a value of 72.4 m/s. Negative value of the tangential velocity indicates that tangential velocity acts in the opposite direction to that of the blade rotation. Figure 15 shows the pathlines colored by the velocity magnitude. Both the front and the isometric views are shown.

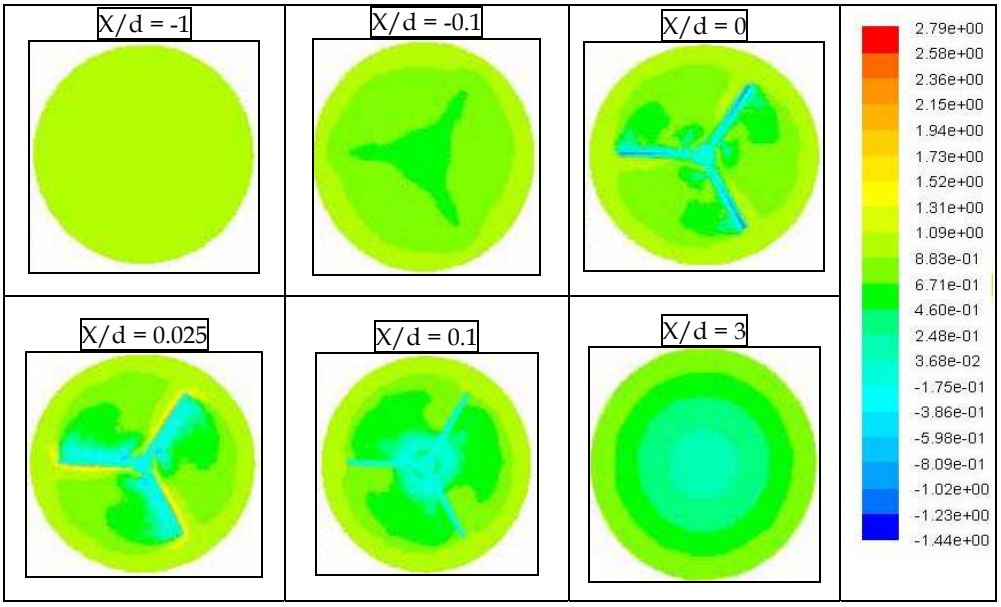

Fig. 11. Normalized axial velocity (Vx/Vo) contours at different x/d locations - TSR=7 and stream velocity V_0 =10 m/s

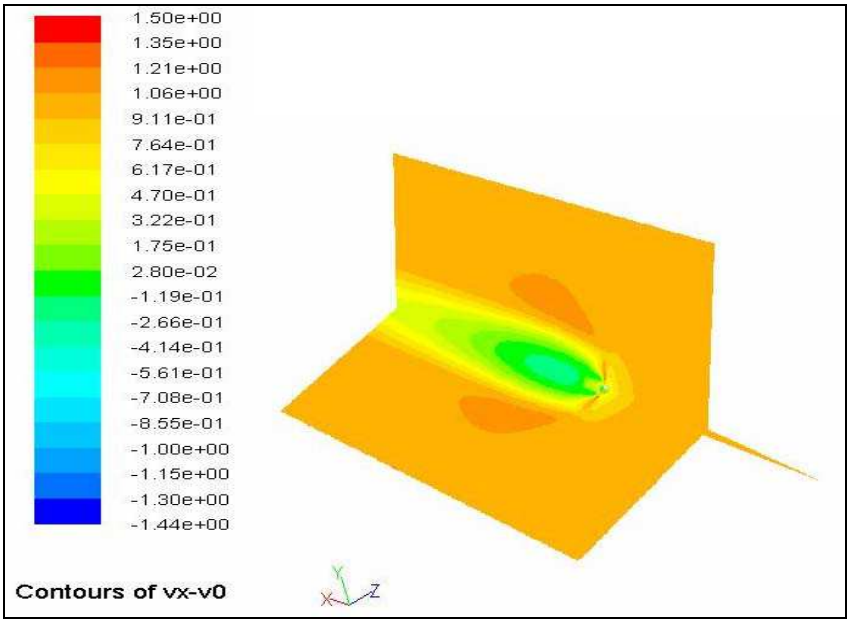

Fig. 12. Wake expansion along the flow at y = 0 inclined plane, which cuts through the turbine blade at angle of 60º to the z-axis.

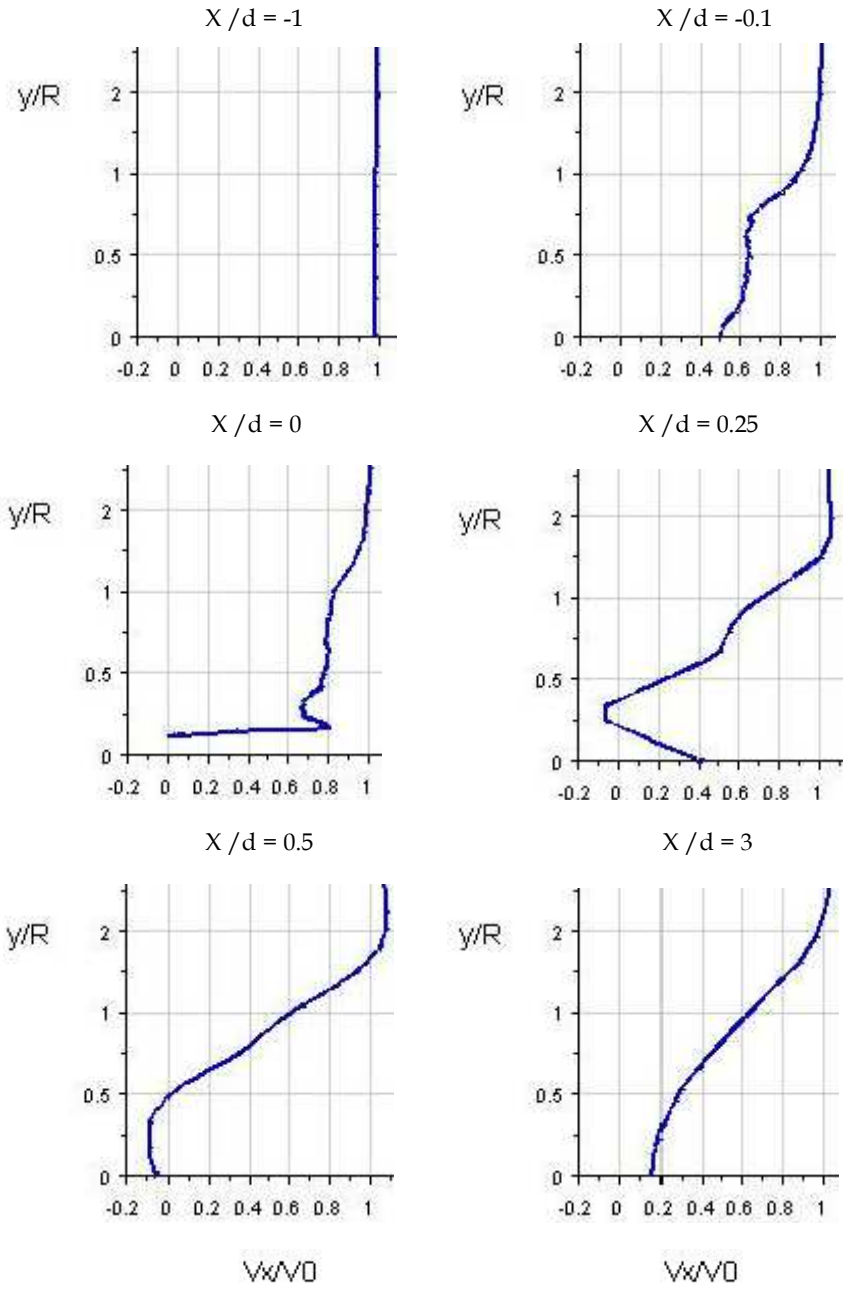

Fig. 13. Normalized axial velocity (VX/Vo) plots along the flow direction

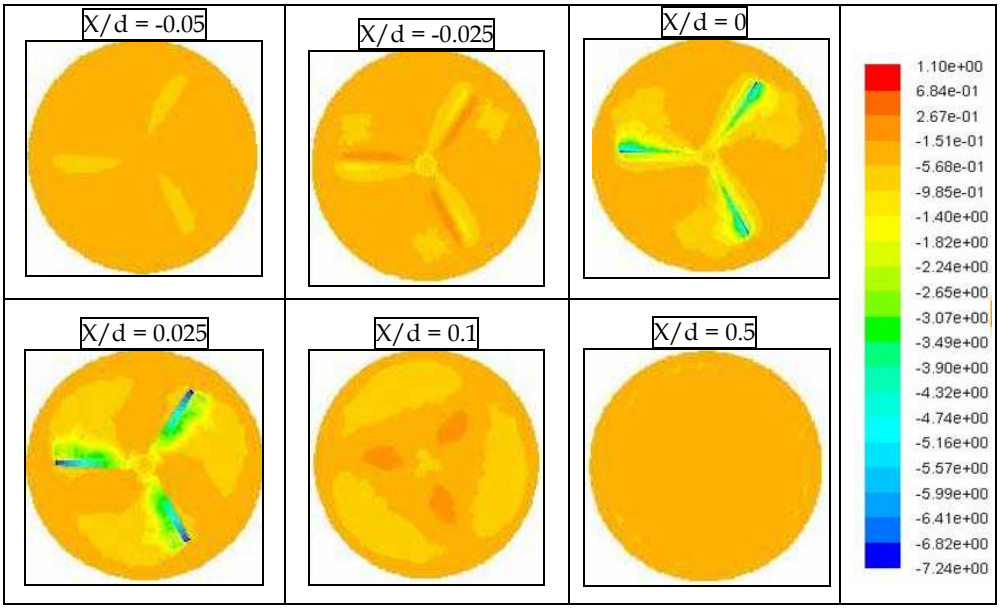

Fig. 14. Normalized tangential velocity contours at different x/d locations - TSR=7 and stream velocity V_0 =10 m/s

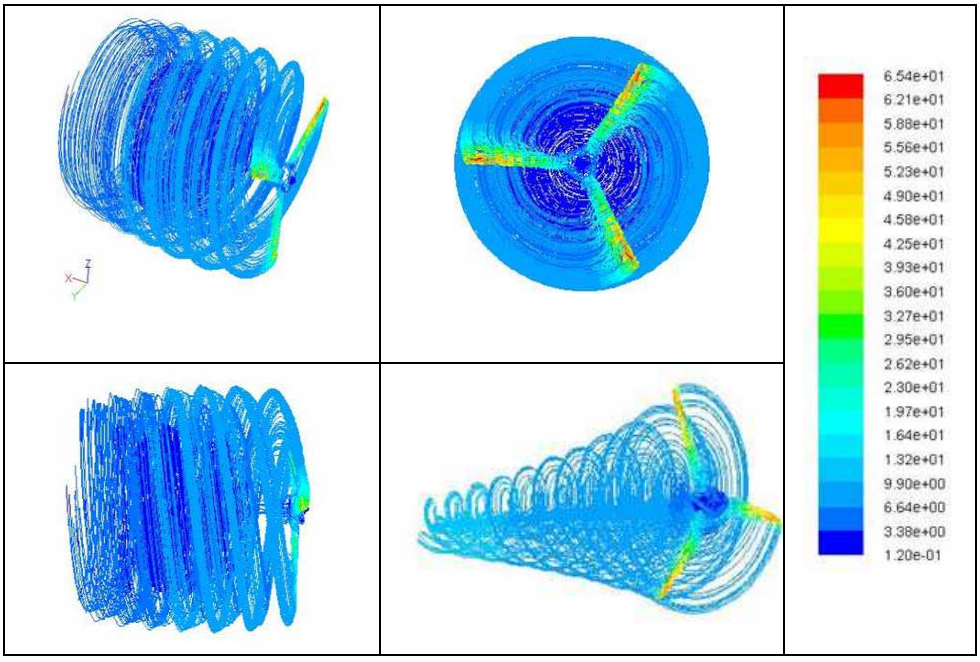

Fig. 15. Pathlines colored by the velocity magnitude (m/s) – Isometric and front views

The power coefficient was determined using the induction factor a. The induction factor was first determined from the velocity profiles before and after the wind turbine and then the power coefficient was calculated. The results of the variation of the power coefficient with the tip speed ratio are presented in Figure 16. The CFD results of the power coefficient were compared to the NREL Unsteady Aerodynamics Experimental data (Acker and Hand, 1999). It is noted that the results presented in Figure 16 are obtained with a normalized TSR value between 3 and 9. The value of the normalized TSR was increased by keeping the wind speed constant at 10 m/s and increasing the rotational speed of the wind turbine or the angular velocity Ω (rad/s). The CFD results shows that the maximum value of power coefficient is 40% with a normalized value of TSR = 7. At this condition the wind turbine will produce approximately 7 KW of mechanical shaft power. For the experimental study the turbine achieves a pick efficiency of approximately 36% at tip speed ratio of approximately 5.5 in controlled wind tunnel environment. The simulated power coefficient curve has a similar trend like other typical turbines. The results also show a good agreement with the experimental data.

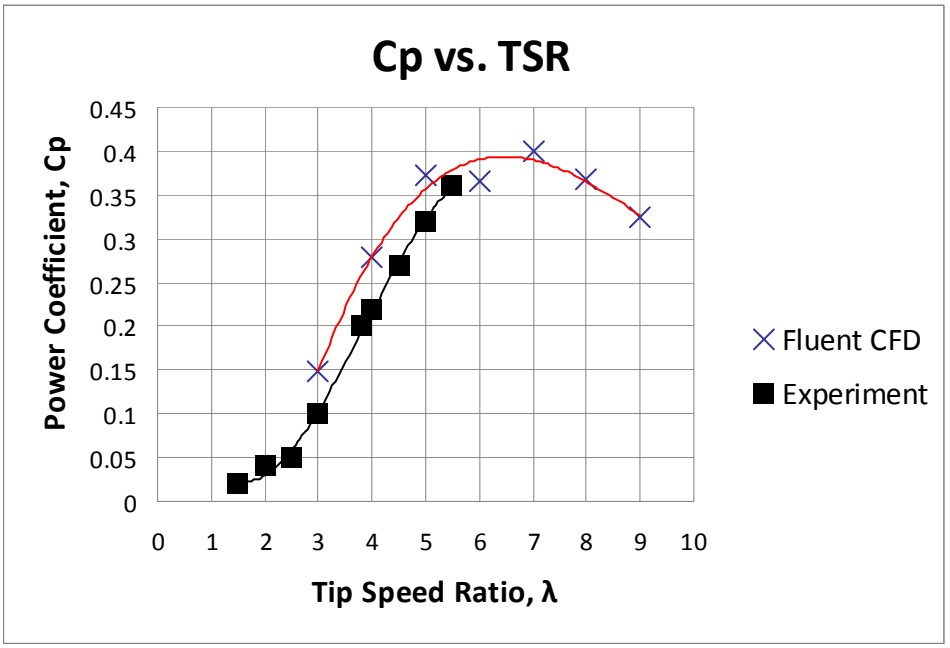

Fig. 16. Variation of the power coefficient with the tip speed ratio - Comparison of the CFD results with experiment

3. Conclusions

This chapter is divided in two parts: the first part is a review of wind energy in general and the second part concerns the use of CFD Reynolds Average Navier Stokes simulations to get better understanding of wind turbine blades aerodynamics and to determine the wind turbine power coefficient. Several issues were addressed in the first part of this chapter

including the role of wind energy in the development of sustainable energy systems and the reasons for switching to renewable energy sources; the fundamental concepts of wind turbines systems (type of wind turbines, wind turbine components, the design of wind turbine, wind turbine power, power coefficient of performance, energy and torque); the wind characteristics such as wind power density, wind shear and turbulence and their effect of wind turbine performance; the flow structure in the near and far wake; design of wind turbines, wind farm and information data about top commercial wind turbines.

The second part if this chapter presents a three dimensional modeling of fluid flow around horizontal axis wind turbine using Reynlolds Average Navier Stokes method. Due to periodicity, only one third of the turbine rotor was modeled in the moving reference frame. The simulations were performed using the k-ε turbulence model and finite-volume method. The axial, radial and tangential velocity contours, pressure distribution on the turbine blades, near and far wake characteristics, turbulence intensity and the power coefficient were obtained in this study. The results from the computations were quite satisfactory and they can represent a good foundation for future work. The results obtained will help better understanding of the flow field past the rotating blades, the pressure distribution on the wind turbine blades, flow structure in the near and far wakes, determine the power extracted from the wind power and to optimize the performance of the wind turbines. The CFD results for the power coefficient versus the normalized tip speed ratio were compared to experimental data and found to be in good agreement. The CFD-RANS method can be used as a CFD tool for computing performances and loads on wind turbine blades and as analysis tool for single turbine and wind farm design.

Future works should include higher performance computers in order to create much more elements in the computational grid, use more sophisticated meshing techniques to create hexahedral elements and refinement of boundary layer for achieving more accurate results, use k-ω SST turbulence model for RANS method and perform more extensive unsteady computation analysis using large eddy simulations (LES).

4. References

Acker, T.; Hand, M., "Aerodynamic Performance of the NREL Unsteady Aerodynamics Experiment (Phase IV) Twisted Rotor", AIAA-99-0045, Prepared for the 37th AIAA Aerospace Sciences Meeting and Exhibit, Reno, NV, January 11-14, 1999, p. 211-221.

Burton T., Sharpe D., Jenkins N. and Bossanyi E, Wind Energy Handbook, John Wiley & Sons Ltd: Chichester, 2001.

Carcangiu, C.E., Sorensen, J.N., Cambuli, F., Mandas, N., CFD-RANS analysis of the rotational effects on the boundary layer of wind turbine blades, Dansk Vindkraftkonference 2007, Trinity, Snoghoj, Fredericia, 25- 27 April 2007

European Wind Energy Agency, VV.AA. Annual report. Technical report, EWEA, European Wind Energy Agency, 2006

Hansen M.O.L, Aerodynamics of Wind Turbines. Rotors, Load and Structures. James & James: London, 2000.

Hartwanger, D. and Horvat, A., 3D Modeling of a wind turbine using CFD, NAFEMS UK Conference, Cheltenham, United of Kingdom, June 10-11, 2008

Hau E, Wind turbines. Springer: Berlin, 2000.

Kang S. and Hirsch C, Features of the 3D flow around wind turbine blades based on numerical solutions. In Proceedings of EWEC 06: Copenhagen, 2001.

Rohden R, Revolutionary blade design. Wind Blatt, the Enercon Magasine, 03, 2004
Sorensen J.N. and Shen W.Z, Numerical modeling of wind turbine wakes. Journal of Fluid Engineering, 124:393–9, 2002.
Sorensen N.N. Johansen J. and Conway S, CFD computations of wind turbine blade loads during standstill operation. KNOW–BLADE Task 3.1, Technical Report R-1465, Riso National Laboratory Roskilde - DK, June 2004.
Sorensen N.N. et al. Tip shape study. Technical Report R-1495, Riso National Laboratory Roskilde - DK, January 2005.
International Energy Agency, VV.AA, Wind energy annual report, Technical report, IEA, International Energy Agency, 2006.
World Wind Energy Association (WWEA), World Wind Energy Report, 2009, http://www.wwindea.org

Paths to Sustainable Energy

Edited by Dr Artie Ng

ISBN 978-953-307-401-6
Hard cover, 664 pages
Publisher InTech
Published online 30, November, 2010
Published in print edition November, 2010

The world's reliance on existing sources of energy and their associated detrimental impacts on the environment- whether related to poor air or water quality or scarcity, impacts on sensitive ecosystems and forests and land use - have been well documented and articulated over the last three decades. What is needed by the world is a set of credible energy solutions that would lead us to a balance between economic growth and a sustainable environment. This book provides an open platform to establish and share knowledge developed by scholars, scientists and engineers from all over the world about various viable paths to a future of sustainable energy. It has collected a number of intellectually stimulating articles that address issues ranging from public policy formulation to technological innovations for enhancing the development of sustainable energy systems. It will appeal to stakeholders seeking guidance to pursue the paths to sustainable energy.

How to reference

In order to correctly reference this scholarly work, feel free to copy and paste the following:

Chaouki Ghenai and Nevzat Sargsyan (2010). Wind Energy, Paths to Sustainable Energy, Dr Artie Ng (Ed.), ISBN: 978-953-307-401-6, InTech, Available from: http://www.intechopen.com/books/paths-to-sustainable-energy/wind-energy-

INTECH
open science | open minds

InTech Europe
University Campus STeP Ri
Slavka Krautzeka 83/A
51000 Rijeka, Croatia
Phone: +385 (51) 770 447
Fax: +385 (51) 686 166
www.intechopen.com

InTech China
Unit 405, Office Block, Hotel Equatorial Shanghai
No.65, Yan An Road (West), Shanghai, 200040, China
中国上海市延安西路65号上海国际贵都大饭店办公楼405单元
Phone: +86-21-62489820
Fax: +86-21-62489821